Optical Kossel line study of an aligned monodomain sample of a cholesteric phase: Temperature evolution of the Kossel diagram

R. J. Miller,[1] H. F. Gleeson,[1,*] and J. E. Lydon[2]
[1]*Department of Physics and Astronomy, Manchester University, Manchester M13 9PL, United Kingdom*
[2]*Department of Biochemistry and Molecular Biology, University of Leeds, Leeds LS2 9JT, United Kingdom*
(Received 5 August 1998)

In the preceding paper, the optical Kossel diagram of an aligned monodomain sample of a cholesteric phase was studied. The Kossel diagram reported was a single annular broad ring containing fine detail which depended on the polarization conditions of the incident light. With crossed polarizers there was a pattern of four spiral arms and a central more intense band. The pattern was shown to be consistent with the analytical treatment of the selective reflection of light by the cholesteric phase of Oldano *et al.* This paper extends the investigation to explore the way in which the appearance of the Kossel ring changes with the temperature and hence the pitch of the sample. Measurements of key positions on the Kossel rings and the features contained within them are shown to be in good agreement with theory. The measurement of the pitch of the cholesteric phase from the Kossel diagrams is also described. [S1063-651X(99)03302-4]

PACS number(s): 61.30.Eb, 78.20.Ci, 78.20.Fm

INTRODUCTION

The optical Kossel technique offers a method of studying the structures of materials with repeat distances of the order of visible wavelengths. Such systems include the cholesteric phase, the twist grain boundary phases, and the blue phases I and II. In the preceding paper [1] we described a Kossel line study of an aligned single domain sample of a cholesteric phase at a particular temperature. The helicoidal axis of the sample coincided with the axis of the microscope used to form the Kossel diagrams. The Kossel diagram was composed of a single annular ring and when viewed between crossed polarizers fine detail comprising four spiral arcs and a more intense central band was observed. This fine detail and the way in which it varied as the polarization state of the incident light and the orientation of the analyzer were changed appeared to be in full agreement with the earlier experimental and analytical studies of the reflection of light by cholesteric structures by other workers, particularly by Dreher and Meier [2], Sugita *et al.* [3], Takezoe *et al.* [4], Miraldi *et al.* [5], and Oldano *et al.* [6].

This paper describes the way in which the fine structure of the Kossel ring changes with the temperature of the sample. Variation in temperature results in concurrent changes in the helical pitch, refractive indices, and birefringence of the cholesteric material. The temperature variation of the helical pitch is generally significant, while that of the refractive indices and birefringence is minor. The Kossel diagrams of the aligned sample therefore also vary with temperature, providing a more general test of the degree to which these experimental observations fit their theoretical description. It is in principle possible to make quantitative measurements from Kossel diagrams of liquid crystals, as has been done extensively for blue phases [7]. In particular, it should be possible to measure the helical pitch directly from the Kossel ring as well as deducing the ordinary and extraordinary refractive indices of the system in special circumstances. Measurements of the refractive indices and pitch of the system studied have been made using conventional techniques and these are compared with measurements made directly from the Kossel diagrams of the aligned cholesteric system. Hence, the way in which the Kossel diagrams may be used to measure the refractive indices and pitch of a system is described.

EXPERIMENT

The apparatus used to generate the Kossel diagrams has been described in detail elsewhere [8]. The geometry of Kossel line formation in the case of cholesteric liquid crystals is shown in Fig. 1. Monochromatic light of wavelength 488 nm was generated with an Argon ion laser and made to converge on the sample using a high numerical aperture microscope objective. The selectively reflected light was then collected using the same lens. The Kossel diagram is the diffraction pattern which is observed in the back focal plane of the microscope objective. In general a Kossel diagram consists of a family of lines, each of which corresponds to a particular Bragg reflection. The lines appear as projections of circles onto a plane, giving either circles, ellipses, or straight lines, depending on the orientation of the corresponding reciprocal lattice vector. In the case reported here only one reflection is involved, the first-order Bragg reflection from the helicoidal repeat in the cholesteric structure. Since the sample is aligned with its helicoidal axis parallel to the optic axis of the microscope, this results in a single centrally placed annular ring. If the experiment was concerned with a single incident wavelength and a single value of refractive index, a single Kossel ring at the Bragg angle would result. The broadening of the reflection from a line into an annulus arises from the variation of refractive index with the polarization state of the light.

The liquid crystal sample studied was the thermochromic mixture TM533 provided by Merck, Ltd. [9]. The sample

*Author to whom correspondence should be addressed. Electronic address: Helen.Gleeson@man.ac.uk

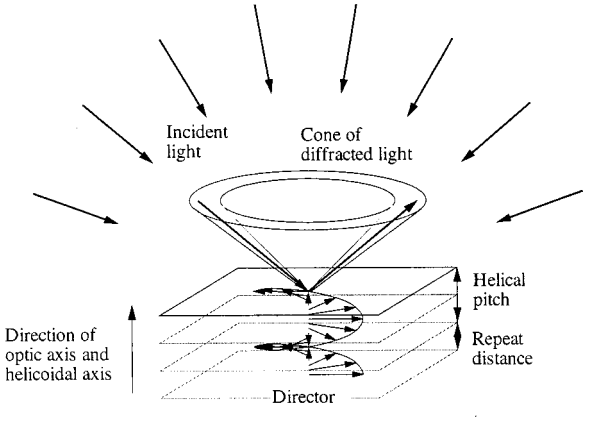

FIG. 1. The geometry of Kossel line formation for cholesteric liquid crystals. The sample is illuminated with a highly convergent cone of monochromatic laser light via the high numerical aperture objective. The selectively reflected light is then collected using the same objective lens and the pattern which is brought to a focus in the back focal plane is the Kossel diagram of the system. In general, a Kossel diagram consists of a pattern of lines, with the shapes of conic sections, each of which corresponds to a particular Bragg reflection from the periodic structure of the sample. For the special case of a monodomain cholesteric sample viewed down the helicoidal axis the Kossel diagram consists of a centrally placed annulus as shown.

was held between two glass substrates that had been treated for homogenous alignment, providing a well aligned sample of the cholesteric material with the helicoidal axis normal to the substrates. The sample was held in a Linkam THMS 600 hot stage and the temperature controlled by a Linkam TMS 91 controller to an accuracy of $\pm 0.1\,^{\circ}\mathrm{C}$. The Kossel diagrams were recorded using a CCD camera connected to a computer equipped with a frame grabber, which made it possible to make measurements directly from them.

In order to examine the quality of measurements made from the Kossel diagrams it was necessary to measure the pitch and refractive indices of TM533 independently. The refractive indices of the material were found to within 0.5% by measuring the angle of total internal reflection of monochromatic light from a homogeneously aligned sample sandwiched between two glass prisms, whose temperature was controlled to 0.1 °C. The technique used to determine refractive index is essentially the same as used in an Abbé refractometer. Measurements of the refractive indices were made at 488.0, 589.3, and 670.0 nm to allow compensation for the dispersion of the thermochromic material. The refractive index of the material between these wavelengths was found by fitting Sellmeier's equation

$$n^2 = 1 + \frac{A\lambda^2}{\lambda^2 - \lambda_1^2},$$

to the experimental data, where A and λ_1 are fitting constants, n is the refractive index, and λ is the wavelength of the light. The cholesteric pitch was determined from the reflection spectra at normal incidence which, for a sample illuminated by white light, comprised of a broad band centred at λ_0 and of width $\Delta\lambda$. The spectral features are defined by the equations

$$\lambda_0 = \bar{n}p \quad \text{and} \quad \Delta\lambda = \Delta n p,$$

where p is the pitch of the cholesteric helix, $\bar{n}=$ is the average refractive index of the material, and Δn is the birefringence. The fitted refractive indices were then used to determine the pitch of the system to within ± 2 nm from measurements of λ_0. The temperature of the sample was again maintained using a hot stage with an uncertainty of $\pm 0.1\,^{\circ}\mathrm{C}$.

THEORETICAL BACKGROUND

Modeling the selective reflection of light by cholesteric structures has proved to be a difficult mathematical problem and there has been a succession of papers dealing with this subject, culminating in the analytical approaches adopted by Dreher and Meier [2] and Oldano *et al.* [6]. In these treatments the state of the light within the sample is described as a superposition of two Bloch wave eigenmodes, each representing an elliptically polarized ray traveling through the medium with a periodicity that matches its local environment. Where a mode is ''stable'' it is transmitted, and where it is ''unstable,'' it is reflected. The map showing the ranges of incidence angle (θ_i) and wavelength (λ) or functions of these two parameters for which the two Bloch waves are stable or unstable (i.e., where selective reflection occurs) has been called the stability chart. Two different (but more or less topologically identical) forms of this plot have been proposed. In the Dreher and Meier form [2], the parameter m is plotted against the reduced wavelength λ/d, where m is defined by the equation $m = \mu \sin\theta_i$, μ is the refractive index and d is the periodicity of the system. Oldano *et al.* [6] used a slightly different form of the chart, where m^2 is plotted against the reduced frequency ω_r, defined as $p/2\lambda$ (p is the pitch of the helicoidal structure and the periodicity d is half the pitch for cholesteric systems). The Kossel diagrams presented here are discussed in terms of the Oldano plot, reproduced in part in Fig. 2. The experimental observations shown in Fig. 3 correspond to the series of vertical sections through the first order reflection band.

The variation in appearance of the Kossel ring predicted from the stability chart can be summarized as follows. The previous investigation of the Kossel diagram at a single temperature [1] is represented by the vertical section through the reflection band labeled *XX* in Fig. 2. This lies within the ω_r range where the reflection band has three distinct parts, the two outer regions where only one of the eigenmodes is reflected and a central region where both are reflected.

At higher ω_r values (beyond those investigated in this study) the first order band divides into three with the two outer single mode bands diverging from the central band where mode mixing has occurred. For the bands corresponding to the second and higher order reflections, this splitting is present over the whole ω_r range of the reflections [6].

At lower values of ω_r the central two mode band (which corresponds to the central more intense ring within the annulus) narrows and eventually becomes a line of zero width for normal rays (i.e., when $m=0$). In contrast, the two one mode shoulders only narrow slightly and the reflection band is still broad at $m=0$. When the ω_r value is about 0.3, the half width of the band approaches its radius and the central

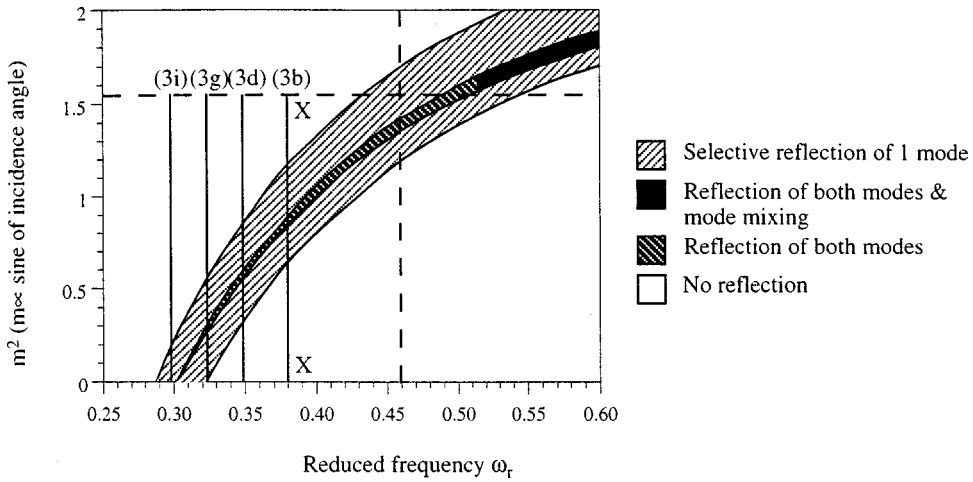

FIG. 2. Part of the stability chart of Oldano *et al.* [6]. In the form of the stability chart used by Oldano *et al.*, the vertical axis is m^2 (where $m = n \sin \theta_i$, n is the refractive index, and θ_i is the incidence angle). The horizontal axis is the reduced frequency ω_r, defined to be $p/2\lambda$. There are four distinct areas shown in the chart. (a) The unshaded areas, where both modes are stable (i.e., where the wave reflections have real roots) and where there is no selective reflection. (b) Regions shown in light shading where one wave is stable and the other is unstable (i.e., there is one real and one imaginary root) where one mode is reflected and the other is transmitted. (c) Regions shown in dark shading where both modes are unstable and where they are reflected independently. (d) Regions shown in solid black where both modes are reflected and where mode mixing occurs. Note that the stability chart is not universal in the sense that the positions of the various boundaries depend on the value of the corresponding refractive indices. The dashed lines on the figure correspond approximately to the experimental limits of the investigation reported here, limited in the horizontal direction by the material and wavelength of light used, and in the vertical direction by the numerical aperture of the apparatus. The labeled solid vertical lines mark approximately the positions on the chart corresponding to various Kossel diagrams in Fig. 3.

hole in the Kossel annulus disappears giving a solid circle. The appearance of the fine detail within the Kossel ring depends on the polarization conditions used, as described in the preceding paper [1].

RESULTS AND DISCUSSION

The Kossel diagrams. Figure 3 shows the appearance of the Kossel diagrams recorded over a range of temperatures within the cholesteric sample. The section of the transmission band across the stability chart which corresponds to certain of the Kossel diagrams is indicated by the appropriate label on Fig. 2. Note that because Fig. 2 is drawn for a system with refractive indices that differ from the system studied experimentally here, the positions marked that correspond to specific Kossel diagrams are only approximate. There is clearly a gratifying degree of correspondence between the overall appearance of the observed annuli and the patterns implied by the stability chart. Note that the positions of the boundaries (i.e., both the position and the thickness of the reflection band) in the stability chart depend on the values of the refractive indices and birefringence of the cholesteric phase at each temperature. The narrowing of the inner, more intense ring as the two mode region narrows with decreasing ω_r and the disappearance of the central hole in the Kossel annulus at a value of $\omega_r \sim 0.3$ occur as expected.

The Kossel band in the stability chart becomes progressively wider as ω_r increases. The apparent narrowing of the observed Kossel rings for high ω_r values is an artifact caused by the limited numerical aperture of the objective lens, cutting off the higher angle part of the ring. The limit is marked approximately by the horizontal dashed line in Fig. 2.

A factor discussed by Dreher and Meier [2] and Oldano *et al.* [6], but not shown explicitly on the stability chart, is the polarization state of the light. In the preceding paper [1] it was demonstrated that the observed pattern of four spiral arms on the Kossel annulus, viewed under crossed linear polarizers, is compatible with both these analytical approaches. It further agrees with the earlier experimental investigations reported by these authors using conventional reflection studies with parallel beams of incident light.

As the incident ray becomes closer to the normal (i.e., as the value of m^2 approaches zero), the single mode reflection changes from more or less linear to elliptical and ultimately it becomes circularly polarized. This leads to the observed loss of contrast of the spiral arms as viewed with crossed polarizers apparent in the micrographs shown in Fig. 3.

The pitch and refractive indices. The refractive indices of the thermochromic material are shown in Fig. 4. It is interesting to note the slight increase in the refractive index parallel to the director on approaching the smectic *A* phase from the cholesteric which is apparent in Fig. 4. This effect, not mirrored in the refractive index perpendicular to the director, is due to the pretransitional influence of the underlying smectic-*A* phase. The occurrence of cybotactic groups would have a larger influence on the parallel refractive indices than the perpendicular ones, as observed. Figure 5 shows the pitch of the cholesteric sample as a function of temperature as measured from the selective reflection spectra. The divergence of the pitch as the cholesteric to smectic-*A* phase transition is approached is evident at low temperatures.

Due to the seminumerical nature of the theory of Oldano *et al.* they do not obtain an analytical relation between the pitch and the locus of the edges of the reflection band, which would allow pitch measurements to be made directly from the Kossel diagrams. However, analysis of their theoretical

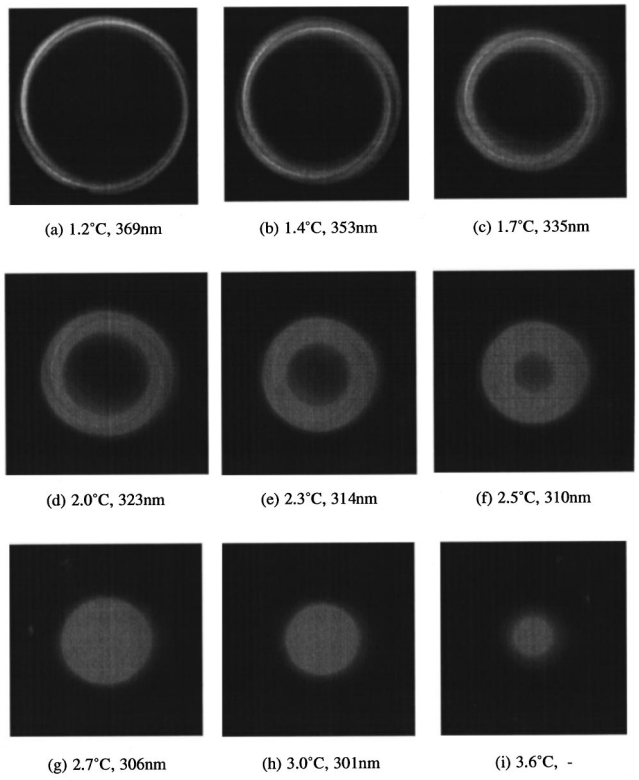

FIG. 3. The experimental Kossel diagrams. The temperature and pitch (deduced from selective reflection spectra) are indicated for each of the diagrams. Note the following. (1) the pattern of spiral arcs disappears progressively as the pitch decreases (m tends to zero)—this occurs as the polarization state of the single mode shoulders progresses from linear to elliptical to circular. (2) The inner, more intense ring, narrows as the two mode region narrows with decreasing ω_r. (3) The central hole in the Kossel ring disappears at an ω_r value around 0.3. (4) The Kossel ring appears to narrow at high m values. This is an artifact caused by the limited numerical aperture of the objective lens used marked by a horizontal dashed line in Fig. 2.

stability plot, reproduced in Fig. 2, suggests that the information can be represented in a simpler form. To first approximation the behavior of the reflection angle of light of a specific wavelength is given by Bragg's law

$$\lambda = 2nd \sin \phi,$$

where λ is the wavelength of the incident light in free space, n the relevant refractive index of the material, d the repeat distance (half the helical pitch p), and ϕ is the conventional Bragg angle of the light. At normal incidence the value of n will be n_o or n_e on either edge of the band corresponding to first-order reflections. Further, Bragg's law will be obeyed for the ordinary ray at other angles of incidence. However, the value of the refractive index for the extraordinary ray will vary with angle away from the normal incidence condition, so that Bragg's law as written above with a single value of n will not describe the situation.

It is instructive to redraft the stability plot produced by Oldano *et al.* in a form where the application of Bragg's law is more apparent. Replacing $\lambda = p/2\omega_r$, $d = p/2$, and $\sin \phi$

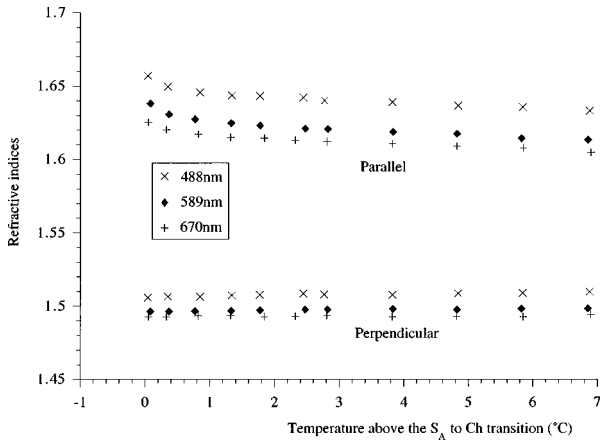

FIG. 4. The refractive indices of TM533 as a function of the temperature above the cholesteric to smectic-A phase transition, measured at wavelengths of 488, 514, and 670 nm. The temperature range shown is well below the isotropic phase transition temperature.

$= \cos \theta$, where θ is the angle of light propagation to the layer normal, the Bragg's law relationship may be rearranged to give

$$n \cos \theta = \frac{1}{\omega_r}.$$

Hence, substituting in $\cos \theta = \sqrt{1 - \sin^2 \theta}$ and $m = n \sin \theta$ one obtains

$$m^2 = n^2 - \frac{1}{4\omega_r^2} = n^2 - \frac{\lambda^2}{p^2}, \tag{1}$$

i.e., there is a linear relationship between m^2 and λ^2/p^2 with a gradient of -1. Figure 6 shows the stability chart redrawn with variables λ^2/p^2 and m^2. Fitting Eq. (1) to data extracted from the stability plot it is found that the higher frequency, lower angle edge of the primary reflection band provides an excellent fit with $n^2 \equiv \varepsilon_\perp$, the relative dielectric permittivity perpendicular to the molecules. This is in keeping with the electric field of the light being perpendicular to the molecular

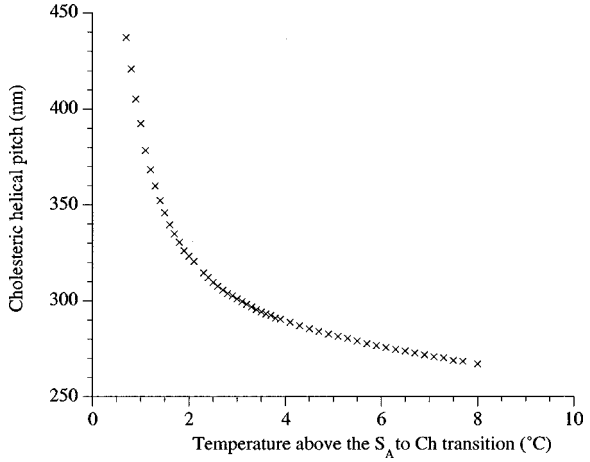

FIG. 5. The temperature dependence of the cholesteric pitch of TM533, determined from the reflection spectra at normal incidence.

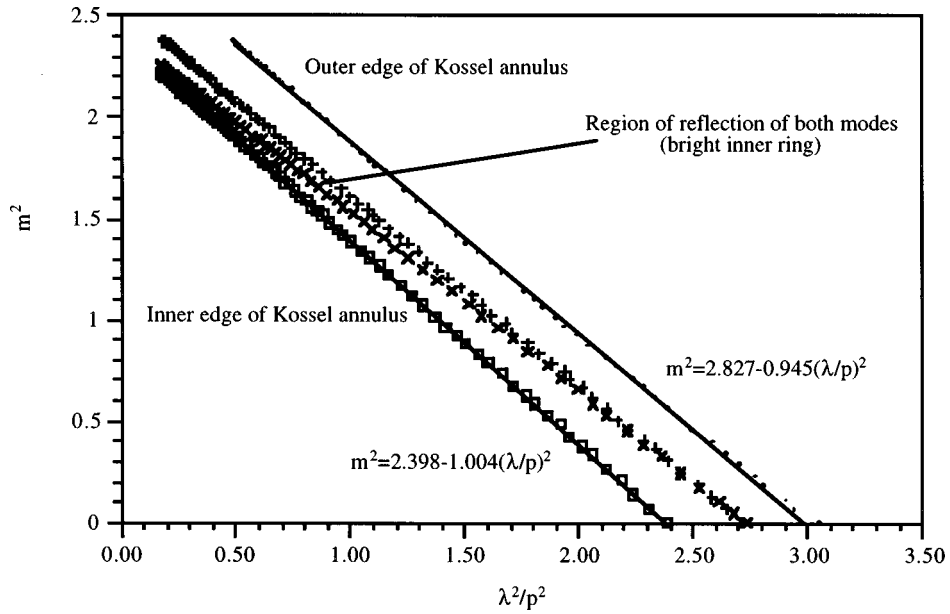

FIG. 6. A portion of the Oldano stability chart redrawn with variables that show Bragg's law more clearly, according to Eq. (1). The straight lines are fits to Eq. (1) with fitting parameters as indicated.

director at this edge of the reflection band. At the alternative edge of the reflection band the situation is more complex since the extraordinary refractive index varies with angle. Nonetheless, the intersection of the outer edge of the band with the horizontal axis corresponds to the case of normal incidence and thus gives a value for the square of the extraordinary refractive index $n_{\|}$. Further, Bragg's law implies that the line corresponding to reflection of the ordinary ray should have a gradient of -1 in Fig. 6, which it does. The gradient of the second line, corresponding to the outer edge of a Kossel diagram, i.e., the extraordinary refractive index, does not have a gradient of -1, as may be expected since it will deviate from Bragg's law.

The parameter m is readily measured from the Kossel diagrams by taking the radial position of the edges of the annuli in the diagrams and scaling the result such that the radius of the diagram is equivalent to the numerical aperture of the optical system. Figure 7 shows a plot of m^2 (measured from the Kossel diagrams) versus λ^2/p^2 (with p deduced from the selective reflection spectra) according to Eq. (1) for the thermochromic material TM533. Clearly both the edges of the bright annulus and the edges of the second band structure within the annulus all follow straight lines. Further the gradient of the line corresponding to the ordinary refractive index fits well to -1. The slight deviation from the straight line fit that is apparent for the system can be attributed partly

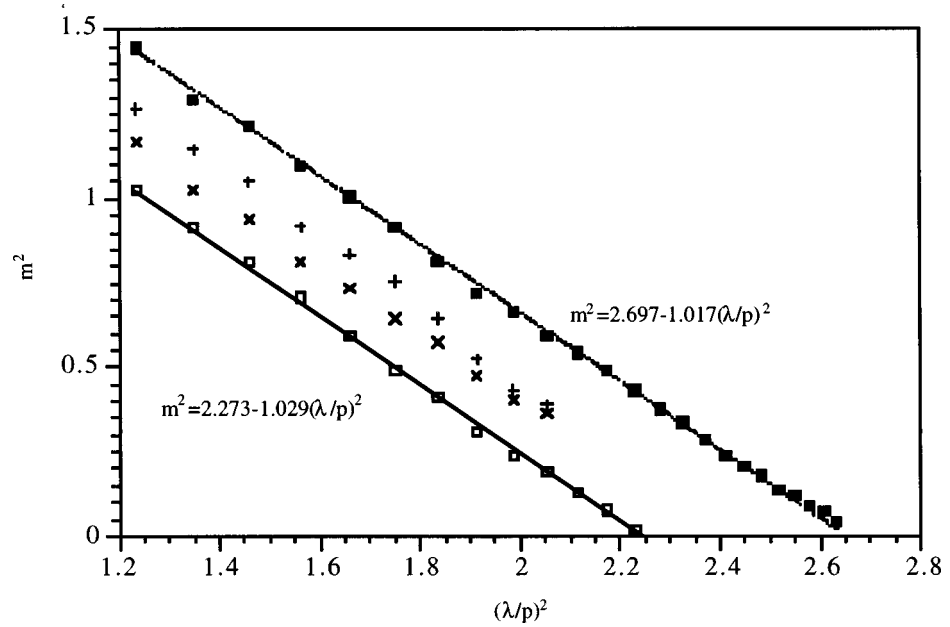

FIG. 7. A plot of m^2 versus λ^2/p^2 according to Eq. (1) for TM533. The straight line fits lines corresponding to the outer and inner edges of the Kossel diagram were constrained to pass through n_o^2 and n_e^2 on the x axis, as would be expected from Eq. (1).

to the fact that the refractive index of the material is slightly different for all the points, due to the temperature change used to vary the pitch. The fitted values of the refractive index are $n=1.507$ and $n=1.642$ for the lower and upper lines, respectively.

It is instructive to consider the uncertainties that can contribute to the graph presented in Fig. 7. The influence of the temperature dependence of the refractive indices has already been mentioned and makes only a small contribution to the uncertainty of the data. However, Fig. 7 presents a graph of data derived from two different experiments and the major source of uncertainty in the gradient and intercept values arises from the uncertainty in temperature between the two different experiments (m is derived from the Kossel diagram, whereas p is determined from selective reflection experiments, Fig. 5). The temperature in each case is known to $\pm 0.1\,^{\circ}\mathrm{C}$, as has already been mentioned. This extrapolates to an uncertainty in the gradient of the graph of ± 0.05, a significant deviation from Bragg's law. However, this uncertainty is relevant only to the comparison of the two different data sets. If Kossel diagrams alone are used to deduce the pitch of the system, a gradient of -1 can be assumed for the first-order reflections. Then, measurements of m^2 from the position of the inner edge of the Kossel annulus can be used to deduce a value of the pitch, provided the ordinary refractive index is known. Since the wavelength of the illuminating light is known to a high accuracy, this allows the pitch to be deduced directly from the Kossel diagram measurements and a knowledge of n_o. Alternatively, if the illuminating wavelength was changed such that the second-order reflection was also observed, it would in principle be possible to deduce the pitch of the system with no knowledge of the refractive index of the sample, provided dispersion is negligible. This is possible since the values of m^2 at for the first- and second-order reflection orders are related to the pitch and illuminating wavelength by Bragg's law [Eq. (1)], modified to include a factor of $4(2^2)$ for the second-order reflection condition. The equations for the first- and second-order conditions can be thus subtracted to remove the dependence on refractive index from them, allowing the pitch to be deduced directly.

CONCLUSION

Observations of the variation of the Kossel diagram with temperature and hence the pitch of an aligned monodomain sample of a cholesteric phase, viewed along the helicoidal axis, appear to be in complete qualitative and convincing quantitative agreement with the analytical treatments of Dreyer and Meier and of Oldano *et al.* We stress the usefulness of the stability chart in portraying the complexities of the selective reflection process in a readily comprehensible form. Methods of making quantitative measurements of the pitch of a helicoidal system from the Kossel diagrams are also described, providing a way of deducing these parameters experimentally that does not require a complete knowledge of the refractive indices of the system.

ACKNOWLEDGMENTS

The financial support of the EPSRC and the DERA is gratefully acknowledged (Grant No. GR/H/95860). The authors also thank William Deakin for useful discussions.

[1] R. J. Miller, H. F. Gleeson, and J. E. Lydon, preceding paper, Phys. Rev. E **59**, 1821 (1999).

[2] R. Dreher and G. Meier, Phys. Rev. A **8**, 1616 (1973).

[3] A. Sugita, H. Takezoe, Y. Ouchi, A. Fukuda, E. Kize, and N. Goto, Jpn. J. Appl. Phys., Part 1 **21**, 1543 (1982).

[4] H. Takezoe, Y. Ouchi, A. Sugita, M. Hara, A. Fukuda, and E. Kuze, Jpn. J. Appl. Phys., Part 1 **21**, 1390 (1982); H. Takezoe, Y. Ouchi, A. Sugita, M. Hara, A. Fukuda, and E. Kuze, *ibid.* **22**, 1080 (1983).

[5] E. Miraldi, C. Oldano, P. Taverna Valabrega, and L. Trossi, Mol. Cryst. Liq. Cryst. **103**, 155 (1983); E. Miraldi, C. Oldano, P. Taverna Valabrega, and L. Trossi, Jpn. J. Appl. Phys., Part 1 **23**, 802 (1984).

[6] C. Oldano, E. Miraldi, and P. Taverna Valabrega, Phys. Rev. A **27**, 3291 (1983); C. Oldano, *ibid.* **31**, 1014 (1985).

[7] S. Meiboom and M. Sammon, Phys. Rev. A **24**, 468 (1981); D. L. Johnson, *et al.*, Phys. Rev. Lett. **45**, 641 (1980); G. Heppke *et al.*, J. Phys. (France) **50**, 549 (1989).

[8] R. J. Miller, J. E. Lydon, and H. F. Gleeson, J. Phys. (France) **6**, 909 (1996).

[9] Merck, Ltd., Merck House, Poole, Dorset, United Kingdom.